Hindawi
International Journal of Photoenergy
Volume 2023, Article ID 6838533, 12 pages
https://doi.org/10.1155/2023/6838533

Research Article

Investigation on Fluid Flow Heat Transfer and Frictional Properties of Al_2O_3 Nanofluids Used in Shell and Tube Heat Exchanger

Debabrata Barik,[1] **Sreejesh S. R. Chandran**,[2] **Milon Selvam Dennison**,[3] **T. G. Ansalam Raj**,[4] **and K. E. Reby Roy**[5]

[1]*Department of Mechanical Engineering, Karpagam Academy of Higher Education, Coimbatore 641021, India*
[2]*Department of Mechanical Engineering, Eranad Knowledge City Technical Campus, Manjeri, Malappuram, Kerala 676122, India*
[3]*Department of Mechanical Engineering, Kampala International University, Western Campus, Kampala, Uganda 20000*
[4]*Department of Mechanical Engineering, Valia koonambaikulathamma College of Engineering and Technology, Kollam, Kerala 691574, India*
[5]*Space Technology Laboratory, Department of Mechanical Engineering, TKM College of Engineering, Kollam, Kerala 691005, India*

Correspondence should be addressed to Debabrata Barik; debabrata93@gmail.com
and Milon Selvam Dennison; milon.selvam@kiu.ac.ug

Received 14 April 2022; Revised 14 October 2022; Accepted 11 March 2023; Published 31 March 2023

Academic Editor: Yaxuan Xiong

Nanofluids are generally utilized in providing cooling, lubrication phenomenon, and controlling the thermophysical properties of the working fluid. In this paper, nanoparticles of Al_2O_3 are added to the base fluid, which flows through the counterflow arrangement in a turbulent flow condition. The fluids employed are ethylbenzene and water, which have differing velocities on both the tube and the shell side of the cylinders. A shell tube-type heat exchanger is used to examine flow characteristics, friction loss, and energy transfer as they pertain to the transmission of thermal energy. The findings of the proposed method showed that the efficiency of a heat exchanger could be significantly improved by the number, direction, and spacing of baffles. With the inclusion of nanoparticles of 1% volume, the flow property, friction property, and heat transfer rate can be considerably improved. As a result, the Nusselt number and Peclet numbers have been increased to 261 and 9.14*E*+5. For a mass flow rate of 0.5 kg/sec, the overall heat transfer coefficient has also been increased to a maximum value of 13464. The heat transfer rate of the present investigation with nanoparticle addition is 4.63% higher than the Dittus–Boelter correlation. The friction factor is also decreased by about 17.5% and 11.9% compared to the Gnielinski and Blasius correlation. The value of the friction factor for the present investigation was found to be 0.0376. It is hence revealed that a suitable proportion of nanoparticles along with the base fluids can make remarkable changes in heat transfer and flow behavior of the entire system.

1. Introduction

The world of thermal engineering is centered on the term heat exchanger (HX), which is necessary for several industries that are required for heat reduction economically. Hence, the HX with low operational and management costs was designed with operating cooling fluids that extract the generated heat. The shell-tube style HX is recognized for its easiness in design; in general, it comprises the following parts: shell, tube, baffles, and fluids. The shell forms the outermost portion by enclosing all other parts and is liable for carrying the cooling fluids from entry to exit over the tubes. The tube transmits the boiling fluid generated from the system by the cooling fluid, where there is heat transfer among the fluids. Chandran et al. [1] reported that the baffles are arrayed to alter the flow course of the cooling fluid in the HX. These varieties of HX have higher reliability than the other types as they can be operated at high pressure and

possess a higher surface area to volume ratio and effectiveness that can be easily enhanced by accumulating the tubes. In general, the heat transfer calculation by CFD is a complicated process as it requires a computer with more power and space. Hence, the resolving of models is required.

Numerous sorts of cooling fluids implemented in the HXs involve varieties of water, oils, and other organic compounds. Applications of heat exchangers are vast and require a thorough knowledge to cover each aspect. Among the applications, their primary use is in the process industry, mechanical equipment, and home appliances. Heat exchangers are employed for heating district systems extensively. Air conditioners and refrigerators use heat exchangers to condense or evaporate the fluid. Moreover, it also has applications in milk processing to do pasteurization.

Nanofluids are solid-liquid compound materials comprising solid nanoparticles or nanofibers with proportions usually from 1 to 100 nm dispersed in the fluid medium. This type of fluid is not just a plain liquid-solid combination. In comparison, the utmost critical condition of a nanofluid is an agglomerate-free stable suspension over an extended period without instigating any chemical alterations to its base fluid. This could be accomplished by reducing the density amid solids and liquids or by enhancing the viscosity of fluids, i.e., through the addition of nanometer-sized particles and by inhibiting particles from agglomeration, the settling of particles could be avoided [2]. Extensive research has been carried out on alumina-water and TiO_2–water, and the appropriate nanofluid for this study was chosen as Al_2O_3–water nanofluid.

The influences of those cooling fluids on the performance of the heat exchanger were demonstrated through several pieces of research [3]. When heat flux remains constant, the Nu number of Al_2O_3 and TiO_2 increases with a surge of Re number if the experiment is conducted on horizontal circular tube underflow of turbulent nature. They also conveyed that when there is a 3% volume escalation in concentration, there is nearly a 12% decrease in convective heat transfer coefficient. In HX with two pipes by deploying copper oxide/ethylene and alumina/ethylene glycol, Zamzamian et al. [4] resolved that with an upswing in temperature and volume concentration, the heat transfer increases by 50% underflow of turbulent nature with low nanofluid concentration.

Li and Xuan [5] research on comparing the Darcy Weisbach friction factor and the heat transfer coefficient analytically on the Cu-water nanofluids determined an enhancement in heat transfer rate under laminar/turbulent flow. However, the value of f remains constant with an increase in nanofluids. The correlation stated that with an upsurge in volume concentration, heat transfer rate increases [6] based on their study deploying Al_2O_3 nanofluid under the flow of turbulent nature. Wen and Ding [7] indicated that there is progress in the heat transfer rate with improvement in Re number by consuming alumina nanoparticles. In their experiment, the addition of nanoparticles increases the thermal behavior of the nanofluid system which was unravelled by Choi and Eastman [8]. Bahiraei et al. [9] as well as Anoop et al. [10] established that the larger the particles of nanofluid, the lesser would be the rate of heat transfer and added that the shape and size of the nanoparticle with its temperature upset the performance of heat transfer corresponding to nanofluid.

The research conducted by Qi et al. [11] revealed a coincidence between the base fluid characteristics and a negligible pressure drop. The behavior of heat transfer deploying CuO/ethylene glycol nanofluid under natural convection by Abu-Nada and Chamkha [12] showed the escalation in the factor of friction and dynamic viscosity with the order of alumina nanoparticle dispersion in water. [13] illustrated the sizable improvement in heat transfer and turbulence rate when the nanoparticles were added to the base fluids. Namburu et al. [14] had led the experiment with several nanofluids added to the ethylene glycol water and analyzed that the heat transfer performance numerically concluded that nanofluid had enhanced features than base fluid. There was an increase in Re and Nu numbers when the nanoparticle concentration increased [15]. The study conducted by [16] identified that the transport property depends on the size, shape, and volume fraction of nanoparticles. Heris et al. [17] had numerically analyzed and exhibited substantial variation in the thermo-physical characteristics of base fluid when nanoparticles dispersed to it.

The dimpled helical tube was implemented by Suresh et al. [18] for experimentation on friction deploying CuO-water nanofluid to emulate the base fluid [19]. The influence of nanoparticle characteristics on thermal conductivity is listed. Concentrating on the viscosity and conductivity (thermal) as vital properties, Kumar et al. [20] determined that the nanoparticles improve thermal behavior. Nnanna [21] highlighted that at high temperature, the Nu and Re number increases correspondingly with the heat transfer rate of HX.

After the intensive literature survey, this work deals with the numerical investigation of the forced convective HX and different flow behavior of fluids and nanoparticles (Al_2O_3) with homogeneous and counterflow arrangements under the flow of turbulent nature. The analysis is done for the different flow rates with and without nanofluid having 36% baffle cut arrangements without inclination similar to the investigation carried out by Irshad et al. [22]. The study also establishes a substantial rise in the heat transfer properties when baffled with different spacing. The hot and cold fluid is considered ethylbenzene, and nanofluids have different velocities on both shell and tube optimum combination.

2. Methodology

2.1. Shell Tube Type Heat Exchanger (STHX). Shell being the wall of STHX comprises a tube arrangement which carries the hot fluid, and corresponding cooling fluid flows along the performance of the baffles in the shell side. The size and length of the shell depend primarily on the number of tubes and their arrangement. Here, the geometry modelling was carried out using ANSYS Space Claim, while the analysis was made using the finite volume method as in Computational Fluid Dynamics (CFD) tool.

This study deals with the estimation of fluid flow and friction properties of a cold fluid added with nanoparticles

Table 1: Physical and chemical properties of ethylbenzene.

Property	Information
Molecular weight	106.17
Color	Colorless
Physical state	Liquid
Boiling point	136.19°C
Melting point	-94.975°C
Density	0.8670
Partition coefficients	4.34
Vapor pressure	7 mmHg
Autoignition temperature	432°C
Flash point	15°C

Table 2: Properties of Al_2O_3 nanoparticles.

Properties	Values
Density	3.69 g/cm^3
Flexural strength	330 MPa
Elastic modulus	300 GPa
Shear modulus	124 GPa
Bulk modulus	165 GPa
Poisson's ratio	0.21
Compressive strength	2100 MPa
Thermal conductivity	18 W/(m.K)
Specific heat	880 J/(Kg.K)

of spherical dimensions in a shell and tube type heat exchanger. Here, ethyl-benzene is used as a hot fluid at a temperature of about 340 K, whereas the cold fluid is of two types, i.e., water and water-Al_2O_3 nanofluid fluid (WANF) at a temperature of 300 K. The tube parameters such as diameter, pitch layout, and counts were determined for this HX [3].

The property of ethylbenzene is flammable and explosive, and ethylbenzene can be dangerous. Vapors can travel to a source of ignition and then flashback. Ethylbenzene can spread fire by floating on water. Inflammatory and poisonous gases can be produced during combustion as given in Table 1.

The studies by Irshad et al. [22] show that pitch arrangement, number, orientation, and spacing of baffles, along with their direction, can extraordinarily alter the overall efficacy of the heat exchanger. In this present study, the triangular pitch has been selected for the tube bundles as it offers better results regarding enhanced surface area per unit length, i.e., maximum tube density. These tubes are generally built as bundles that can be easily dismounted from the tube arrangement (TFD-HE13–STHX Design). The properties of Al_2O_3 nanoparticles are given in Table 2.

The specifications of STHX have been taken from the studies of Irshad et al. [22] and are given in Table 3. The properties of base fluid and nanoparticles are given in Table 4.

The parameters of STHX were chosen according to the Tubular Exchanger Manufacturers Association (TEMA) Standards and were designed as in Figures 1(a) and 1(b).

Table 3: Geometric dimension of STHX.

Specification of STHX	Dimension
The inner diameter of the shell	90 mm
Length of the shell	600 mm
The outer diameter of the tube	20 mm
Number of tubes	7
Tube pitch geometry	30 mm, triangular
Baffle cuts	36%
Baffle spacing	86 mm
Baffle thickness	3 mm
Number of baffles	6

Table 4: Properties of base fluid and nanoparticles.

Properties	Base fluid (water)	Nanoparticle (Al_2O_3)
Density	998.2 kg/m^3	3690 kg/m^3
Thermal conductivity	0.608 W/(m.K)	18 W/(m.K)
Dynamic viscosity	0.001002 kg/(m.s)	—
Specific heat capacity	4182 J/(kg.K)	880 J/(kg.K)

The modelled STHX then meshed initially with a relatively coarser mesh, ending in 58645 elements. This mesh comprised mixed elements of both tetrahedral and hexahedral cells with triangular and quadrilateral faces at the boundaries. It was noted from the previous studies that hexahedral cells are usually advised for a fine capturing of the profile. Hence, for this criterion, a fine mesh was made with maximum care at the wall regions and edges, which are all the regions of high temperature and pressure gradients.

The contours of initially made coarse mesh were analyzed with that of the fine mesh. They observed that the latter mesh resolves better over the regions of high pressure and temperature gradient than the former. The contours depicted a refinement in meshing, particularly at the inlet and outlet regions which would help in the better acquisition of heat transfer and pressure drop. A completely grid-independent model was obtained by interpreting the temperature and pressure gradients.

During fine meshing, the aspect ratio of the elements was maintained the same as that of the aspect ratio of coarse mesh as it possesses only a negligible effect on meshing. The resulting meshed model comprised about 2184591 elements and 4473951 nodes. The different sections of the meshed model are shown in Figure 2.

The main objective of this study is to determine the fluid flow and friction properties along with the alterations in overall heat transfer due to the addition of nanoparticles in the carrier fluid.

2.2. Governing Equation of Motion. For a fluid to flow, it should obey the three governing equations of motion: continuity, momentum, and energy [23]. The three equations of motion are expressed as follows:

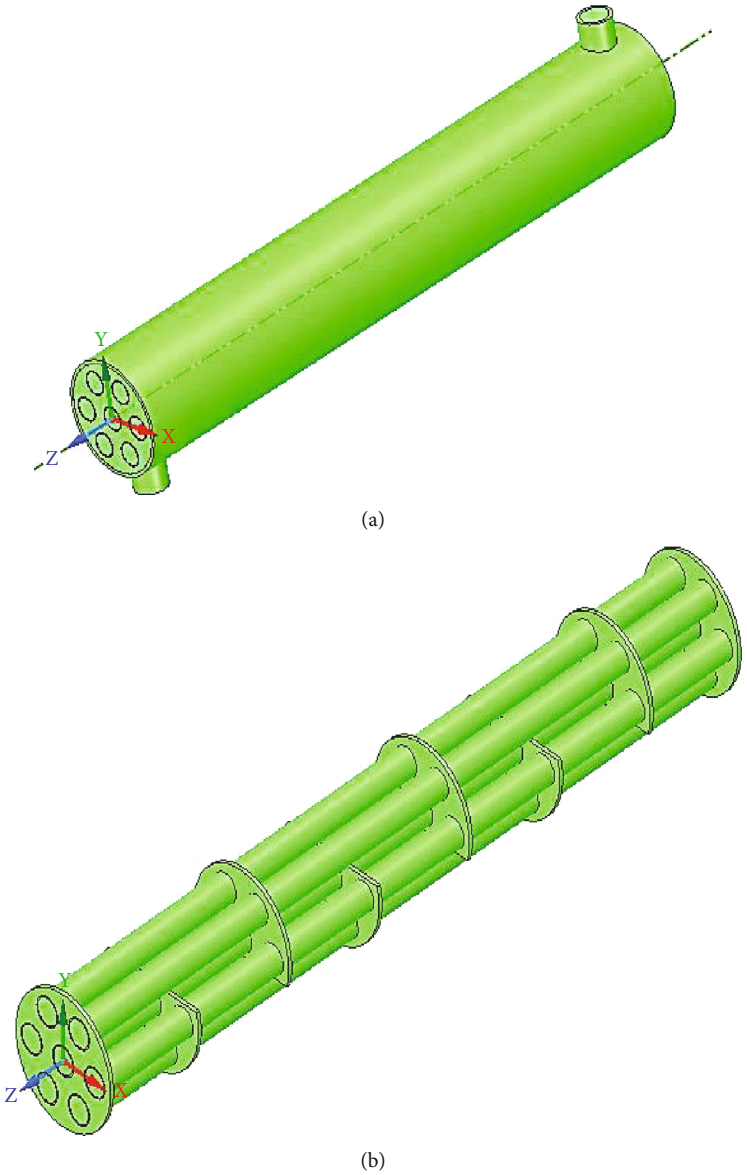

Figure 1: (a) STHX model. (b) Tube bundle arrangement with baffles inside the shell.

Continuity equation:

$$\frac{\partial \rho}{\partial t} + \nabla.(\rho V) = 0. \tag{1}$$

Momentum equation:

$$\rho \frac{DV}{Dt} = \nabla.\tau_{ij} - \nabla_p + \rho F. \tag{2}$$

Energy equation:

$$\rho \frac{De}{Dt} + p\,(\nabla.V) = \frac{\partial Q}{\partial t} - \nabla.q + \varphi, \tag{3}$$

where ρ indicates the density of the fluid, V indicates the velocity of the fluid, τ_{ij} Indicates the viscous stress tensor, p indicates pressure, F indicates body forces in the system, e indicates the internal energy of the fluid, Q indicates heat transfer, t indicates the time, φ indicates dissipation, and $\nabla .q$ indicates heat lost by conduction.

2.3. Data Analysis. The fluid flow properties and the friction properties of nanofluids are determined from the base values of particles used in the heat exchanger. These are determined using the below-mentioned formulae. Anoop et al. [10] provided the density of nanofluid resulting through the mixing of the base fluid, i.e., water and nanoparticles of Al_2O_3 is obtained through in

$$\rho_{nf} = \left[(1-\varphi)\rho_f + \varphi\,\rho_p\right]. \tag{4}$$

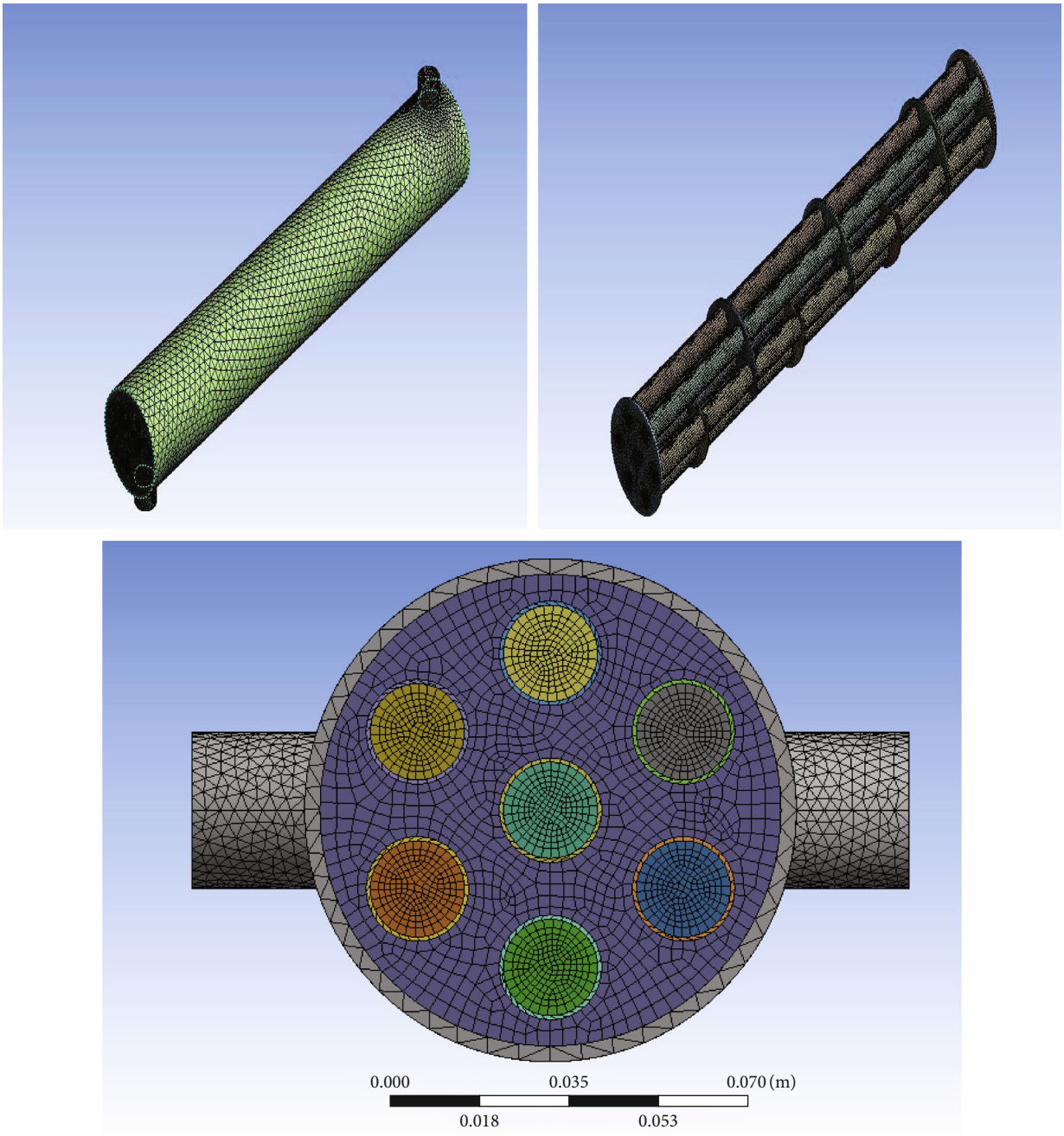

Figure 2: Meshed model.

In the same manner, the specific heat capacity of the nanofluid is given as [10]

$$\left(\rho C_p\right)_{nf} = (1-\varphi)\left(\rho C_p\right)_f + \varphi\left(\rho C_p\right)_p. \tag{5}$$

In Equation (6), the effective thermal conductivity of the resultant nanofluid comprising the solid-liquid mixture can be expressed as [24]

$$K_{nf} = K_f \frac{\left(K + 2K_f - 2\varphi\left(K_f - K\right)\right)}{\left(K + 2K_f + \varphi\left(K_f - K\right)\right)}. \tag{6}$$

Similarly, in Equation (7), the dynamic viscosity of nanofluids with very low volume concentrations of nanoparticles is given by the Einstein model of 1906 [25]:

$$\frac{\mu_{nf}}{\mu_f} = [1 + 2.5\,\varphi], \tag{7}$$

where the subscripts f, p and nf refer to the base fluid, nanoparticles, and nanofluids, respectively. The next parameter that is to be determined is the overall heat transfer rate of the system, which is given as

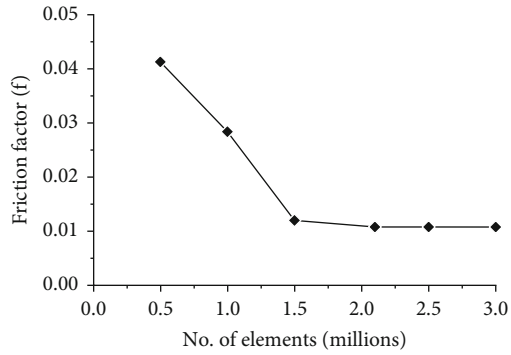

Figure 3: Grid independence study for the turbulent regime.

$$\text{The overall heat transfer rate, } Q = \dot{m} C_{p_{nf}} (T_{\text{out}} - T_{\text{in}}). \quad (8)$$

Here, $\dot{m}$ is the mass flow rate of the nanofluid system, and T_{out} and T_{in} are the outlet and inlet temperatures of the nanofluids. In the case of the friction factor of the system, it is obtained through [26]

$$f_{nf} = 0.961 \ \text{Re}^{-0.375} \varphi^{0.052}. \quad (9)$$

In Equation (9), Re is the Reynolds' number which determines the nature of the flow and is given as [27, 28]

$$\text{Re} = \frac{VD_e}{\vartheta}. \quad (10)$$

The obtained results regarding heat transfer rate and friction factor were then correlated with various models of heat transfer correlations by Dittus–Boelter (Equation (11) and Equation (12)), Gnielinski (Equation (13)), and Blasius (Equation (14)) presented as in the below equations [29, 30].

$$\frac{h_i D_i}{k} = 0.023 \left(\frac{G_i D_i}{\mu}\right)^{0.8} \left(\frac{C_p \mu}{k}\right)^{0.3}, \quad (11)$$

$$Q = h A \Delta T, \quad (12)$$

$$f = (0.79 \ln (\text{Re}) - 1.64)^{-2}, \quad (13)$$

$$f = \frac{0.316}{\text{Re}^{0.25}}. \quad (14)$$

2.4. Grid Independence Test. Grid independence study is considered an important procedure in all CFD analyses. The reason is that the solution which is delivered by the CFD software should be independent of the grid size [1]. This study helps find an optimum point for a suitable, accurate solution for the problem with reduced computational resources. With the help of the obtained optimum mesh, the accuracy of the result would be good enough to get all relevant flow features, its gradient, and so on. Grid-independent study is conducted for the turbulent flow regime for four grid quantities such as 0.5 million, 1 million, 1.5 million, 2 million, 2.5 million, and 3 million.

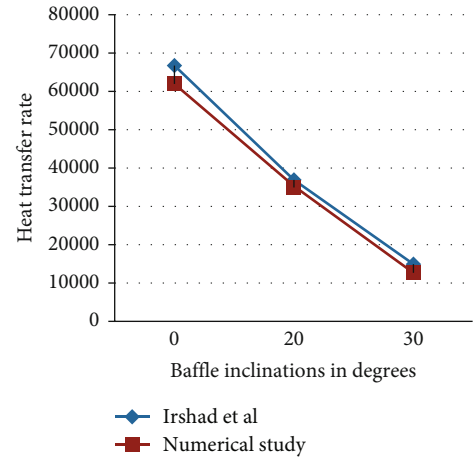

Figure 4: Validation plot of Irshad et al. with numerical study.

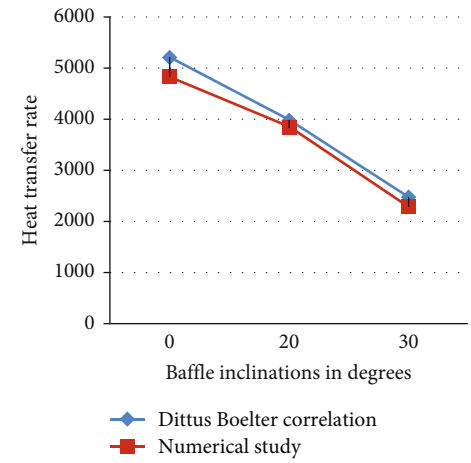

Figure 5: Validation plot of Dittus–Boelter correlation with numerical study.

The friction factor f is taken as one of the parameters to check the grid in dependency. Nusselt number evaluations are employed to discover the fewest number of grids possible without affecting numerical findings, and this procedure is known as the Grid Independence Test. From the study, the 2.1 million grid quantity is selected for further computations since the parameters with the higher mesh density of 60 (width) × 70 (depth) × 600 (length) for the fluid domain do not have appreciable variation as shown in Figure 3. Hence, a comparatively less mesh density is selected for the solid domain.

3. Validation

Figures 4 and 5 show the comparison of the heat transfer rate with baffle inclination plots for Irshad et al. [22], the Dittus–Boelter relation, and the current work. After careful observation, it is revealed that the validated results and the numerical data match pretty well, with maximum variations of 6.9% and 4.63%, respectively.

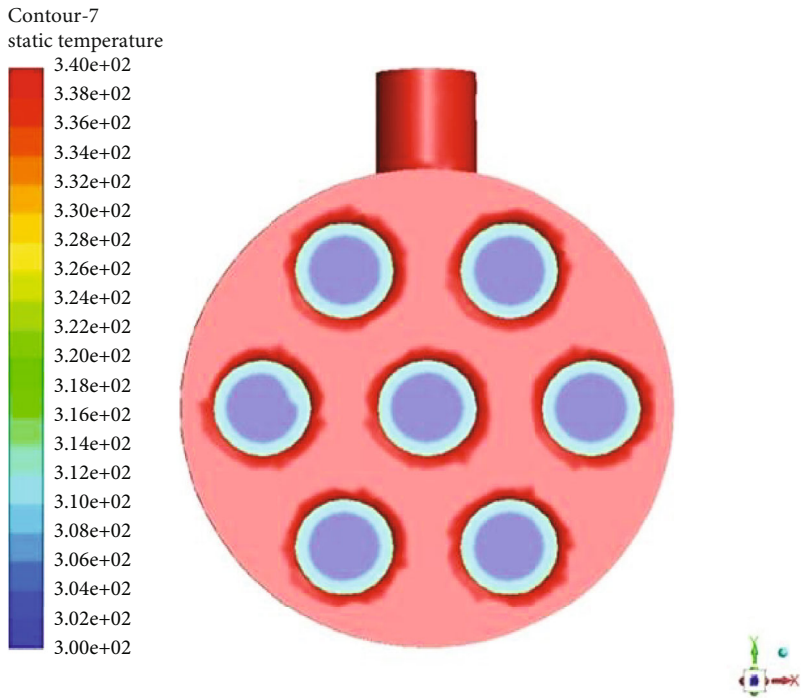

Figure 6: Temperature contour with 1% nanoparticle addition.

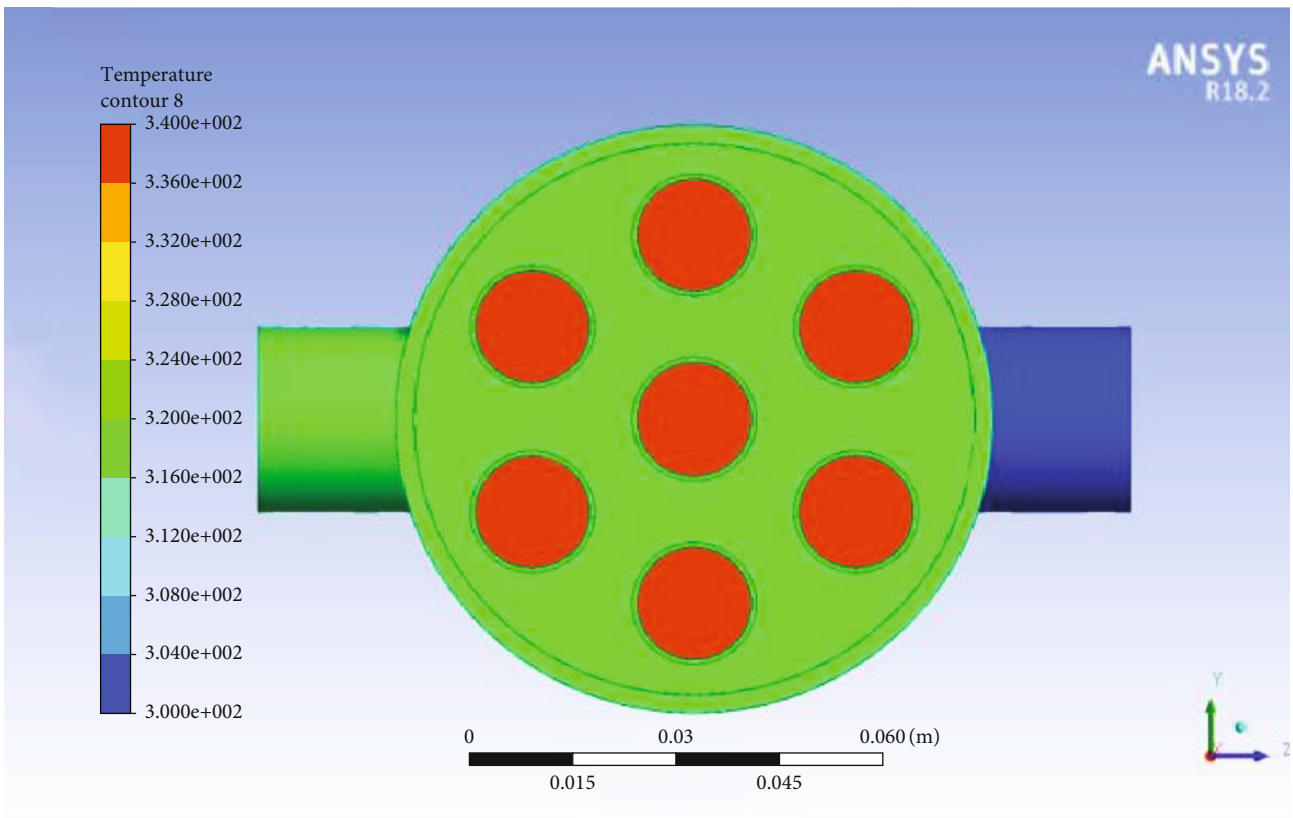

Figure 7: Temperature contour at inlet of the hot fluid.

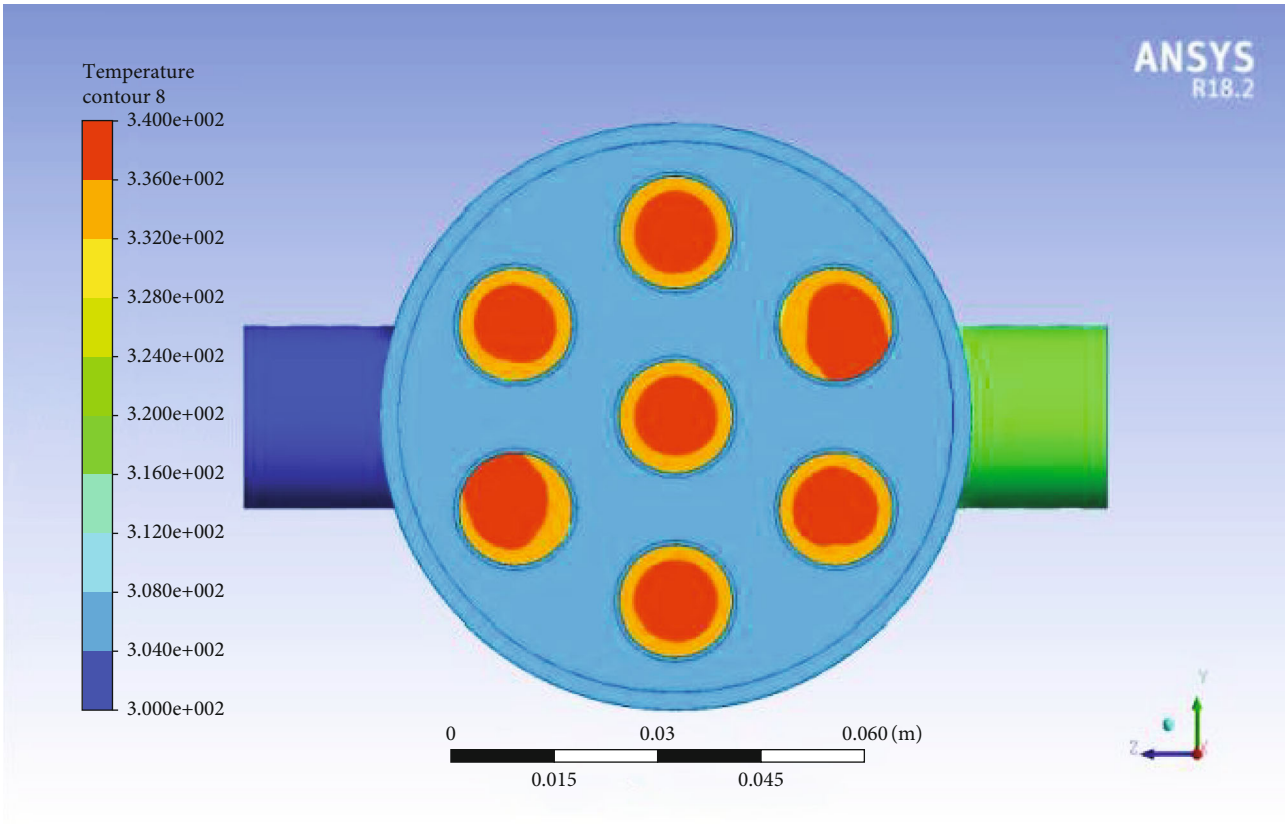

Figure 8: The temperature contour at outlet of cold fluid.

4. Results and Discussions

The present investigation portrays the inclusion of aluminium oxide nanoparticles along with the base fluid water in suitable proportion and the way it enhanced the flow property, friction property, and heat transfer rates is represented in the form of temperature contours, plots, etc.

4.1. Temperature Contour with 1% Nanoparticle Addition. The temperature contour with 1% Al_2O_3 nanoparticle addition is shown in Figure 6. It is clear that the heat gained by the cold fluid is clearly visible from the contour. From the computational domain, it is clear that cold fluid accepts the heat energy at a uniform rate from the hot fluid. Here, turbulence is fair, and heat transfer rate is appreciable.

4.2. Temperature Contour at Inlet and Outlet of Hot Fluid and Cold Fluid. The temperature contour at inlet of the hot fluid is shown in Figure 7. The temperature contour at outlet of cold fluid is shown in Figure 8.

In both inlets and outlets, the contour geometry is good, and heat is transferred perfectly between the boundaries. Even though the flow was a little bit not perfect during initial heat exchange process, it is made up and became uniform during the remaining process.

4.3. Variation of Nusselt Number with Reynolds Number with 1% Alumina. The variation of Nusselt number with Reynolds number with 1% alumina is shown in Figure 9.

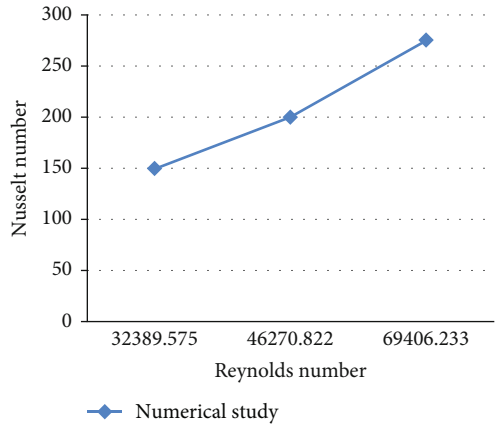

Figure 9: Variation of Nusselt number with Reynolds number with 1% alumina.

Here, the Nusselt number value is increased to 267 because of nanoparticle addition and quite higher without the application of nanoparticle. Nusselt number increases when Reynolds number is increased. Due to greater velocity rate, better heat transfer rates can be achieved. Higher heat transfer rates will lead to a higher Nusselt number.

4.4. Effect of Friction Factor with Reynolds Number for 1% Alumina. The effect of friction factor with Reynolds number for 1% alumina is shown in Figure 10. The effect of friction

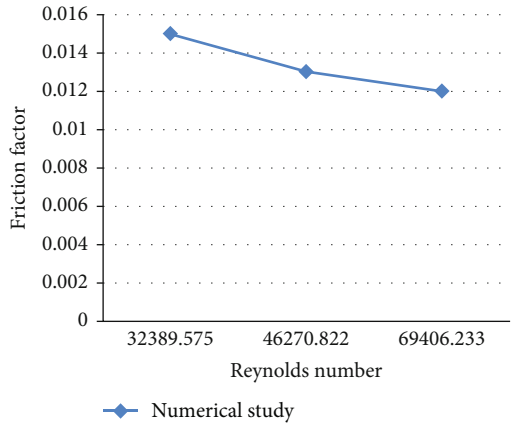

Figure 10: Effect of friction factor with Reynolds number for 1% alumina.

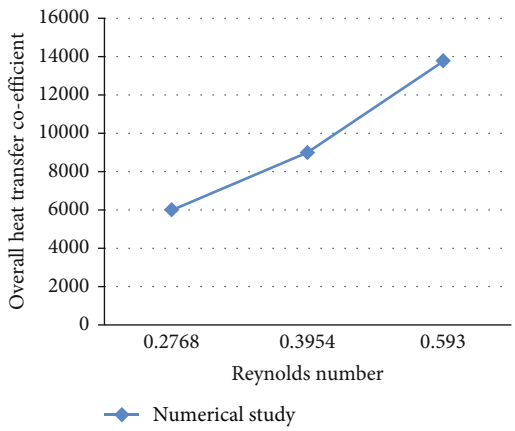

Figure 11: Variation of overall heat transfer coefficient with mass flow rate for 1% alumina.

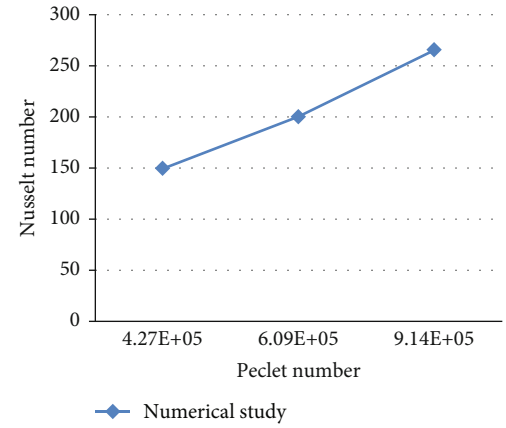

Figure 12: Nusselt number–Peclet number relationship for 1% alumina.

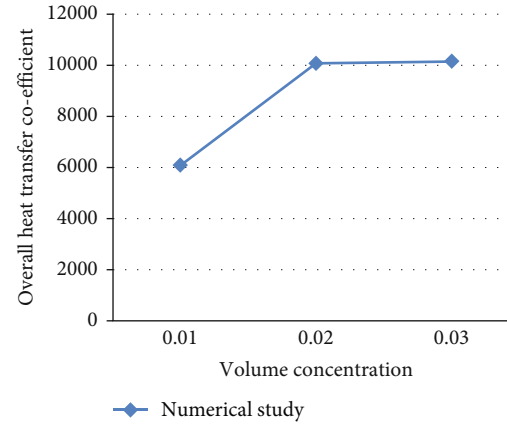

Figure 13: Effect of overall heat transfer coefficient at different concentrations of alumina at 0.7 m/sec velocity.

factor with Reynolds number for 1% alumina is shown in Figure 10. The f value is showing not much variation when Reynolds number is increased, and the value keeps on decreasing also. The above minor change can be neglected.

4.5. Variation of Overall Heat Transfer Coefficient with Mass Flow Rate for 1% Alumina. The variation of overall heat transfer coefficient with mass flow rate for 1% alumina is shown in Figure 11. Here, overall heat transfer coefficient is also found to be at its extreme value when alumina particles are used as nanoparticle. The thermal conductivity of the alumina particles is high. So, this inherent thermal conductivity resulted in a higher U value, and it will result in a higher Nusselt number too. When the mass flow rate is increased to 0.593, the U value will be at the point of 13464 which is quite significant. But the lesser mass flow rates yield a lower U value.

4.6. Nusselt Number–Peclet Number Relationship for 1% Alumina. The effect of Nusselt number with Peclet number for 1% aluminum oxide is shown in Figure 12.

The value of Peclet number and Nusselt number are directly proportional. From the analysis, the Peclet number obtained in all the four flow rates is better. The nanofluid shows greater potential in enhancing the heat transfer process. This is because the suspended ultrafine particles remarkably increase the k value, and Nusselt number is increased. The increase in the value of Peclet number resulted in an increased boundary layer thickness and a slight increase in the friction factor also.

4.7. Effect of Flow Velocity for 1% Alumina. The effect of overall heat transfer coefficient at different concentrations of alumina at 0.7 m/sec velocity is shown in Figure 13.

For a velocity of 0.7 m/sec and at a particle concentration of 1%, a higher overall heat transfer value of 10771 is attained which shows that 1% nanoparticle water combination gave appreciable results.

4.8. Effect of Tube Side Outlet Temperature for 1% Alumina at Different Baffle Inclinations. The effect of tube side outlet temperature for alumina with different baffle inclinations is shown in Figure 14. When baffle inclination increases, tube side outlet temperature also increases. The outlet temperature of the tube outlet is dependent upon the turbulence.

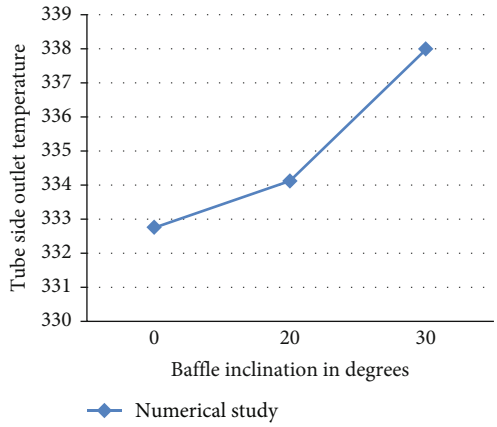

Figure 14: Effect of tube side outlet temperature for alumina with different baffle inclinations.

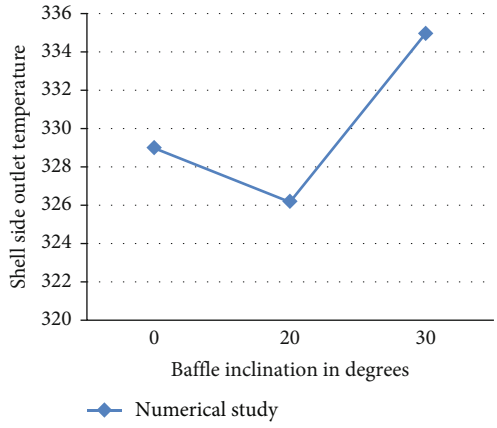

Figure 15: Effect of shell side outlet temperature for alumina with different baffle inclinations.

Tube side temperature reaches a value of 338°C which shows that heat transfer rate is appreciating.

4.9. Effect of Shell Side Outlet Temperature for 1% Alumina at Different Baffle Inclinations. The effect of shell side outlet temperature for alumina with different baffle inclinations is shown in Figure 15.

It is clear from the plot that shell side temperature shows a sudden decrease at 20° baffle inclinations because of lesser aggregation of nanoparticles with the base fluid. The optimum value of shell side temperature is closer to 335 deg. C. The heat transfer characteristics of Alumina-water nanofluid is high at 1% particle concentration.

5. Conclusions

The convective heat transfer performance of alumina-water nanofluid flowing through the shell and tube heat exchanger was investigated numerically, and the effects of nanofluid temperature, concentration and volume flow rates, friction factor, overall heat transfer coefficient, Nusselt number, Peclet number, and shell side and tube side temperatures of nanofluid were investigated. Studies revealed that water along with Al_2O_3 nanoparticles of 1% volume concentration has a better heat transfer rate compared with normal base fluid alone, i.e., only water. All studies have proved that, a substantial increase in the heat transfer rate occurs, followed by an earlier convergence history. It is also understood that addition of nanoparticle positively affects the flow and friction properties of the entire system. The following conclusions have been obtained.

(1) Studies proved that an increase in Reynolds number increases the value of Nusselt number and reaches the peak value of 261 at 1% alumina concentration. The heat exchange rate is very much higher and took reasonable iterations to make the solutions converged. The maximum time taken to complete one iteration is 2 minutes

(2) The quantitative value of the friction factor for the current investigation was observed to be 0.0376 which is not much deviating from the previous investigation which were 17.5% and 11.9% from Gnielinski and Blasius correlations

(3) The thermal conductivity of alumina nanoparticles is very high, and this inherent property enhanced the overall heat transfer coefficient (U) value to 13464 at a mass flow rate of 0.593 kg/sec. When mass flow rate decreases, overall heat transfer coefficient also decreases

(4) The value of Peclet number was seen directly proportional throughout the analysis with Nusselt number because the suspended ultrafine particles remarkably increased the value of thermal conductivity, K, and the Peclet number increases the peak value of $9.14E^{+5}$. The increase in the value of Peclet number resulted in an increased boundary layer thickness and a slight increase in the friction factor also

(5) Studies revealed that when tube side fluid velocity is increased to 0.7 m/sec led to an increase of overall heat transfer to about 10771. It is clear that when tube velocity is increased, U value would tremendously be increased

(6) The optimal values of shell side and tube side outlet temperature are 335 K and 338 K which showed that heat exchange phenomenon is good

(7) It is further concluded that the heat transfer rate can then be enhanced if twisted inserts are accommodated inside the tube side

Nomenclature

Cp: Specific heat at constant pressure, J/(kg.K)
HX: Heat exchanger
K: Thermal conductivity, W/(m.K)
P: Pressure, (N/m^2)
T: Temperature (K)

SBHX: Segmental baffle heat exchanger
STHX: Shell and tube heat exchanger
μ: Dynamic viscosity, Kg/(m.s)
ρ: Density, (kg/m^3)
υ: Kinematic viscosity (m^2/s)
φ: Nanoparticle volume concentration
f: Friction factor
D_e: Equivalent diameter for shell side, (m)
V: Velocity, (m/s).

Data Availability

The data is available in the manuscript.

Disclosure

A preprint of the present work was published [1].

Conflicts of Interest

The authors declare that they have no conflict of interest.

Acknowledgments

The authors sincerely thank the Karpagam Academy of Higher Education (KAHE), India, and Kampala International University, Western Campus, Kampala, Uganda, for providing the necessary facilities to conduct the research.

References

[1] S. S. R. Chandran, D. Barik, T. G. Ansalam Raj, and R. Roy, *Investigation on fluid flow heat transfer and frictional properties of Al_2O_3 nanofluids used in shell and tube heat exchanger*, Research Square, 2020.

[2] V. Sridhara and L. N. Satapathy, "Al_2O_3-based nanofluids: a review," *Nanoscale Research Letters*, vol. 6, no. 1, p. 456, 2011.

[3] B. C. Pak and Y. I. Cho, "Hydrodynamic and heat transfer study of dispersed fluids with submicron metallic oxide particles," *Experimental Heat Transfer an International Journal*, vol. 11, no. 2, pp. 151–170, 1998.

[4] A. Zamzamian, S. N. Oskouie, A. Doosthoseini, A. Joneidi, and M. Pazouki, "Experimental investigation of forced convective heat transfer coefficient in nanofluids of Al_2O_3/EG and CuO/EG in a double pipe and plate heat exchangers under turbulent flow," *Experimental Thermal and Fluid Science*, vol. 35, no. 3, pp. 495–502, 2011.

[5] Q. Li and Y. Xuan, "Convective heat transfer and flow characteristics of Cu-water nanofluid," *Science in China Series E: Technolgical Science*, vol. 49, no. 4, pp. 408–416, 2002.

[6] S. El Bécaye Maïga, C. Tam Nguyen, N. Galanis, G. Roy, T. Maré, and M. Coqueux, "Heat transfer enhancement in turbulent tube flow using Al2O3 nanoparticle suspension," *International Journal of Numerical Methods for Heat & Fluid Flow*, vol. 16, no. 3, pp. 275–292, 2006.

[7] D. Wen and Y. Ding, "Experimental investigation into convective heat transfer of nanofluids at the entrance region under laminar flow conditions," *International Journal of Heat and Mass Transfer*, vol. 47, no. 24, pp. 5181–5188, 2004.

[8] S. U. Choi and J. A. Eastman, *Enhancing thermal conductivity of fluids with nanoparticles*, Argonne National Lab.(ANL), Argonne, IL (United States), 1995.

[9] M. Bahiraei, M. Hangi, and M. Saeedan, "A novel application for energy efficiency improvement using nanofluid in shell and tube heat exchanger equipped with helical baffles," *Energy*, vol. 93, pp. 2229–2240, 2015.

[10] K. B. Anoop, T. Sundararajan, and S. K. Das, "Effect of particle size on the convective heat transfer in nanofluid in the developing region," *International Journal of Heat and Mass Transfer*, vol. 52, no. 9-10, pp. 2189–2195, 2009.

[11] C. Qi, T. Luo, M. Liu, F. Fan, and Y. Yan, "Experimental study on the flow and heat transfer characteristics of nanofluids in double-tube heat exchangers based on thermal efficiency assessment," *Energy Conversion and Management*, vol. 197, article 111877, 2019.

[12] E. Abu-Nada and A. J. Chamkha, "Effect of nanofluid variable properties on natural convection in enclosures filled with a CuO-EG-water nanofluid," *International Journal of Thermal Sciences*, vol. 49, no. 12, pp. 2339–2352, 2010.

[13] J. Buongiorno, "Convective transport in nanofluids," *Journal of Heat Transfer*, vol. 128, no. 3, pp. 240–250, 2006.

[14] P. K. Namburu, D. K. Das, K. M. Tanguturi, and R. S. Vajjha, "Numerical study of turbulent flow and heat transfer characteristics of nanofluids considering variable properties," *International Journal of Thermal Sciences*, vol. 48, no. 2, pp. 290–302, 2009.

[15] A. M. Ardekani, V. Kalantar, and M. M. Heyhat, "Experimental study on heat transfer enhancement of nanofluid flow through helical tubes," *Advanced Powder Technology*, vol. 30, no. 9, pp. 1815–1822, 2019.

[16] K. Subramani, K. Logesh, S. Kolappan, and S. Karthik, "Experimental investigation on heat transfer characteristics of heat exchanger with bubble fin assistance," *International Journal of Ambient Energy*, vol. 41, no. 6, pp. 617–620, 2020.

[17] S. Z. Heris, M. N. Esfahany, and G. Etemad, "Numerical investigation of nanofluid laminar convective heat transfer through a circular tube," *Numerical Heat Transfer, Part A: Applications*, vol. 52, no. 11, pp. 1043–1058, 2007.

[18] S. Suresh, M. Chandrasekar, and S. C. Sekhar, "Experimental studies on heat transfer and friction factor characteristics of CuO/water nanofluid under turbulent flow in a helically dimpled tube," *Experimental Thermal and Fluid Science*, vol. 35, no. 3, pp. 542–549, 2011.

[19] A. R. Khaled and K. Vafai, "Heat transfer enhancement through control of thermal dispersion effects," *International Journal of Heat and Mass Transfer*, vol. 48, no. 11, pp. 2172–2185, 2005.

[20] N. Kumar, S. S. Sonawane, and S. H. Sonawane, "Experimental study of thermal conductivity, heat transfer and friction factor of Al_2O_3 based nanofluid," *International Communications in Heat and Mass Transfer*, vol. 90, pp. 1–10, 2018.

[21] A. G. Nnanna, "Experimental model of temperature-driven nanofluid," *Journal of Heat Transfer*, vol. 129, no. 6, pp. 697–704, 2007.

[22] M. Irshad, M. Kaushar, and G. Rajmohan, "Design and CFD analysis of shell and tube heat exchanger," *International Journal of Engineering Science and Computing*, vol. 7, pp. 6453–6457, 2017.

[23] M. S. Ajithkumar, T. Ganesha, and M. C. Math, "CFD analysis to study the effects of inclined baffles on fluid flow in a shell

and tube heat exchanger," *International Journal of Research in Advent Technology*, vol. 2, no. 7, pp. 164–175, 2014.

[24] Q. Z. Xue, "Model for effective thermal conductivity of nanofluids," *Physics Letters A*, vol. 307, no. 5-6, pp. 313–317, 2003.

[25] K. Bashirnezhad, S. Bazri, M. R. Safaei et al., "Viscosity of nanofluids: a review of recent experimental studies," *International Communications in Heat and Mass Transfer*, vol. 73, pp. 114–123, 2016.

[26] M. H. Barzegar and M. Fallahiyekt, "Increasing the thermal efficiency of double tube heat exchangers by using nano hybrid," *Emerging Science Journal*, vol. 2, no. 1, pp. 1–10, 2018.

[27] B. Farajollahi, S. G. Etemad, and M. Hojjat, "Heat transfer of nanofluids in a shell and tube heat exchanger," *International Journal of Heat and Mass Transfer*, vol. 53, no. 1-3, pp. 12–17, 2010.

[28] J. Koo and C. Kleinstreuer, "Laminar nanofluid flow in microheat-sinks," *International Journal of Heat and Mass Transfer*, vol. 48, no. 13, pp. 2652–2661, 2005.

[29] K. V. Liu, U. S. Choi, and K. E. Kasza, "Measurements of pressure drop and heat transfer in turbulent pipe flows of particulate slurries," NASA STI/Recon Technical Report N, 89, 1988.

[30] M. Arun, D. Barik, K. Sridhar, and G. Vignesh, "Performance analysis of solar water heater using Al_2O_3 nanoparticle with plain-dimple tube design," *Experimental Techniques*, vol. 46, no. 6, pp. 993–1006, 2022.